Hydrogen Production

DOI: 10.1002/anie.201407208

Charge Polarization at a Au–TiC Interface and the Generation of Highly Active and Selective Catalysts for the Low-Temperature Water–Gas Shift Reaction**

José A. Rodriguez, Pedro J. Ramírez, Gian Giacomo Asara, Francesc Viñes, Jaime Evans, Ping Liu, Josep M. Ricart, and Francesc Illas*

Abstract: *Au atoms in contact with TiC(001) undergo significant charge polarization. Strong metal–support interactions make Au/TiC(001) an excellent catalyst for the low-temperature water–gas shift (WGS), with turnover frequencies orders of magnitude larger than those observed for conventional metal/oxide catalysts. DFT calculations indicate that the WGS reaction follows an associative mechanism with HOCO as a key intermediate.*

Transition-metal nanoparticles dispersed on oxides or carbon supports are among the most frequently used catalysts in the chemical and petrochemical industries. In principle, by selection of the right combination of a metal and a support, the energy necessary for chemical transformations could be reduced substantially and the use of chemical feedstocks optimized.[1] Metal–support interactions can have negative[2,3] or positive[4,5] effects on the catalytic properties of a metal. A major challenge in heterogeneous catalysis is to gain an understanding of metal–support interactions at an atomic level and use them to design highly active and selective catalysts.[1,4,5] In the last decades, great effort has been focused on the study of metal–oxide interactions.[1] However, it has become clear that metal carbides can be excellent supports for the dispersion of metal catalysts.[6–10] The metal carbides have interesting catalytic properties on their own,[11–18] and they can also modify the reactivity of a supported metal through chemical bonding.[8,19] In this study, we investigated the performance of Au/TiC(001) surfaces as catalysts for the water–gas shift reaction ($CO + H_2O \rightarrow H_2 + CO_2$; WGS). The WGS is a key process in the industrial production of hydrogen.[20,21] Commercial catalysts for the WGS usually involve mixtures of Fe–Cr and Cu–Zn oxides, which are used at temperatures of 620–770 and 470–525 K, respectively.[20] These catalysts normally require lengthy and complex activation steps before usage. There is a general desire to find WGS catalysts that are active at relatively low temperatures (< 470 K).[20] Metal-carbide-based catalysts meet this criterion,[6,14,17,18] but there are serious concerns about their stability and selectivity.[14,18] Many metal carbides are sensitive to O_2 or oxygen-containing molecules in the reaction feed.[11,14,18] On the other hand, metal carbides can be very active in the cleavage of the C–O bond in carbon monoxide[11,22] and, in the presence of hydrogen, hydrogenate the produced C atoms to yield methane or higher alkanes.[10,13,15,16,23] Our study indicates that the 1:1 metal-to-carbon ratio in TiC lends stability to this carbide substrate and prevents the cleavage of C–O bonds. Strong metal–support interactions make Au/TiC(001) a highly active and selective catalyst for the low-temperature WGS reaction.

Figure 1 shows the WGS activity of clean TiC(001) and Au/TiC(001) surfaces as a function of Au coverage. We found that the clean TiC(001) surface was able to catalyze the WGS, in agreement with the predictions of previous DFT calculations.[17] In fact, at 450 K, TiC(001) displays a WGS activity larger than that of Cu(111), a typical benchmark in WGS studies.[24] Metallic Au does not catalyze the WGS.[26] However, the addition of Au to TiC(001) produces a drastic increase in the WGS activity of the system. A maximum in the production of H_2 and CO_2 was observed at $\theta_{Au} \approx 0.15$ ML. After this point, there was a gradual decrease in the WGS activity of Au/TiC(001). STM studies have shown that at a coverage of 0.1 ML, a large fraction of the Au particles exhibit a height of approximately 0.2 nm with respect to the carbide substrate (see Figure S1 in the Supporting Informa-

[*] Dr. J. A. Rodriguez, Dr. P. J. Ramírez, Dr. P. Liu
Chemistry Department, Brookhaven National Laboratory
Upton, NY 11973 (USA)
E-mail: rodrigez@bnl.gov
Dr. P. J. Ramírez, Prof. J. Evans
Facultad de Ciencias, Universidad Central de Venezuela
Caracas 1020A (Venezuela)
G.-G. Asara, Prof. J. M. Ricart
Departament de Química Física i Inorgànica
Universitat Rovira i Virgili
C/Marcel·lí Domingo s/n, 43007 Tarragona (Spain)
G.-G. Asara, Dr. F. Viñes, Prof. F. Illas
Departament de Química Física and IQTCUB
Universitat de Barcelona
C/Martí i Franquès 1, 08028 Barcelona (Spain)

[**] The research at BNL (Chemistry Department, National Synchrotron Light Source, Center for Functional Nanomaterials) was financed by the US Department of Energy (DOE), Office of Basic Energy Science (DE-AC02-98CH10086). This research has been supported by the Spanish MINECO (grants CTQ2011-29054-CO2-01/BQU and CTQ2012-30751) and, in part, by Generalitat de Catalunya grants 2014SGR97, 2014SGR199, and XRQTC. INTEVEP and IDB financed the research carried out at UCV. G.-G.A. thanks the Universitat Rovira i Virgili for supporting his predoctoral research. F.V. thanks the MINECO for a postdoctoral Ramón y Cajal grant (RYC-2012-10129). F.I. acknowledges additional support through an ICREA Academic Award for excellence in research. Computational time at the MareNostrum supercomputer was generously provided by the Barcelona Supercomputing Center through a grant from Red Española de Supercomputación.

Supporting information for this article is available on the WWW under http://dx.doi.org/10.1002/anie.201407208.

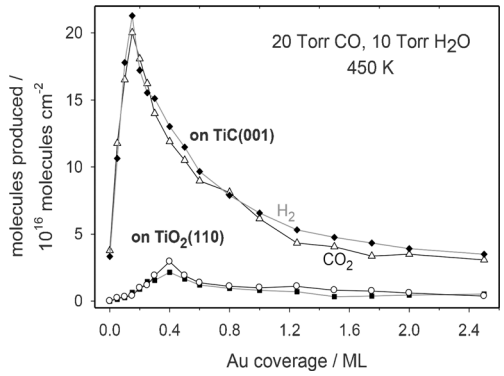

Figure 1. WGS activity of Au/TiC(001) and Au/TiO_2(110) as a function of Au coverage. The reported values for the production of H_2 (filled symbols) and CO_2 (empty symbols) were obtained after exposing the catalysts to CO (20 Torr) and H_2O (10 Torr) at 450 K for 5 min. ML = monolayer.

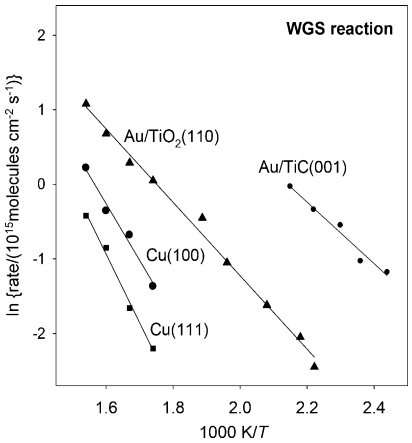

Figure 2. Arrhenius plots for the WGS on Cu(111), Cu(100), Au/TiO_2(110), and Au/TiC(001) catalysts (CO: 20 Torr; H_2O: 10 Torr). Surfaces of metallic Au are not active for the WGS reaction. The data for Cu(111), Cu(100), and Au/TiO_2(110) were taken from Refs. [26, 27]. The coverage of Au on TiO_2(110) and TiC(001) was 0.4 and 0.15 ML, respectively. At these coverages, maximum catalytic activity was observed for Au/TiO_2(110) and Au/TiC(001).

tion).[8,19] These small particles are two-dimensional (i.e. form a single Au layer) and have a diameter below 0.6 nm.[8,19] The Au atoms in these particles are in direct contact with the C sites of the TiC(001) substrate undergoing charge polarization,[25] which shifts electrons towards upcoming molecules (see Figure S2) and enhances their chemical reactivity.[8,9,19] At coverages above 0.2 ML, the gold forms predominantly three-dimensional particles on TiC[7,8,26] (i.e. the Au atoms exposed to the reactants are not electronically modified by interactions with the carbide support), and the chemical reactivity of the system decreases.[8,19] In XPS experiments on the partial dissociation of water on Au/TiC(001) ($H_2O \rightarrow OH + H$), we found extremely high reactivity for surfaces that had a gold coverage below 0.2 ML (see Figure S3). This observation is quite interesting because extended surfaces and isolated nanoparticles of gold do not dissociate the water molecule.[27] Upon the dissociative adsorption of water on Au/TiC(001) systems ($\theta_{Au} < 0.2$ ML), we observed a narrow Au $4f_{7/2}$ peak in the XPS spectrum, with a binding-energy shift of 0.7–0.8 eV with respect to clean Au/TiC(001) (see Figure S3), which is consistent with the formation of $Au(OH)_x$ compounds on the surface. These compounds are active species for the WGS reaction on Au/oxide catalysts.[21,28]

In Figure 1, we compare the WGS activity of a series of Au/TiC(001) and Au/TiO_2(110) surfaces with similar coverages of the admetal. At temperatures of 550–625 K, Au/TiO_2 is known to be a very good catalyst for the WGS,[28,29] with an activity that is higher than that of Cu/ZnO,[30] which is used as an industrial WGS catalyst.[20] The results in Figure 1 indicate that Au/TiC(001) is a much better low-temperature WGS catalyst than Au/TiO_2(110). This observation is corroborated by the data shown in the Arrhenius plots in Figure 2. The apparent activation energy for the WGS process decreases from (18 ± 2) kcal mol^{-1} on Cu(111) to (10 ± 3) kcal mol^{-1} on Au/TiO_2(110) and (8 ± 2) kcal mol^{-1} on Au/TiC(001). The apparent activation energy on Au/TiO_2(110) is close to that found on Au/TiO_2 powders (11 kcal mol^{-1}).[21,28] At relatively low temperatures (< 470 K), Au/TiC(001) exhibits a WGS activity that is observed on copper surfaces and on Cu/oxide or Au/oxide catalysts (oxide = TiO_2, ZnO, CeO_2, MgO) only at elevated temperatures (> 500 K).[29,30]

From the data points in Figure 2, we estimated turnover frequencies (TOFs) for Au/TiC(001) on the assumption that all gold atoms in the catalyst were involved in the WGS process. This assumption is valid, since STM has shown that at a low coverage of Au (ca. 0.15 ML) the admetal grows to form a substantial amount of 2D islands on TiC(001).[8,19] The estimated TOFs at different temperatures are shown in the top graph in Figure 3. The bottom graph compares TOFs for several catalysts. Again it is clear that Au/TiC(001) is an excellent catalyst for the WGS reaction. At 450 K, the Au/TiO_2(110) surface exhibits a TOF close to that reported for Au/TiO_2 powder catalysts (ca. 0.2 s^{-1}),[21] but much smaller than that observed for Au/TiC(001) (3.2 s^{-1}). Furthermore, a Cu/ZnO$(000\bar{1})$ surface, which is a model for industrial Cu/ZnO catalysts,[30] displays a TOF approximately 3 times smaller than that of Au/TiC(001) in spite of an increase of 125 K in the reaction temperature.

As mentioned above, two important issues when dealing with the use of metal carbides as possible catalysts for the WGS are selectivity and stability.[14–18] In many industrial operations, the WGS is performed under hydrogen-rich conditions with mixtures of $CO/H_2O/H_2$ that come from the reforming of hydrocarbons.[6,14] Under hydrogen-rich conditions, metal carbides, such as Mo_2C, transform CO into methane as a side reaction.[15,22] Indeed, after exposing a Mo_2C(001) surface to a $CO/H_2O/H_2$ mixture, we found products of the WGS and CO methanation (Figure 4). We carried out studies comparing the WGS process on Au/TiC(001) and Au/Mo_2C(001) with $CO/H_2O/H_2$ mixtures. A gold coverage of approximately 0.15 ML was deposited on TiC(001) and on a Mo_2C(001) surface.[13,31] Neither TiC(001) nor Au/TiC(001) produced methane as a reaction product, but only produced CO_2 through the WGS reaction (Figure 4). In general terms, Mo_2C(001) is more active than TiC(001) for the

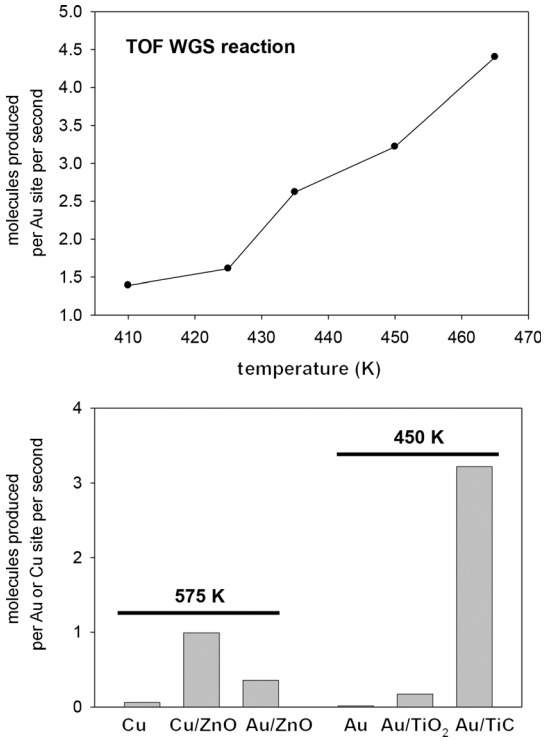

Figure 3. Top: TOFs for the WGS reaction on Au/TiC(001) at different temperatures. Bottom: Comparison of the TOFs for the WGS on Cu(111),[26] Cu/ZnO(000$\bar{1}$),[27] Au/ZnO(000$\bar{1}$),[27] Au(111),[26] Au/TiO_2-(110),[26] and Au/TiC(001). In all cases, the pressures of CO and H_2O were 20 and 10 Torr, respectively.

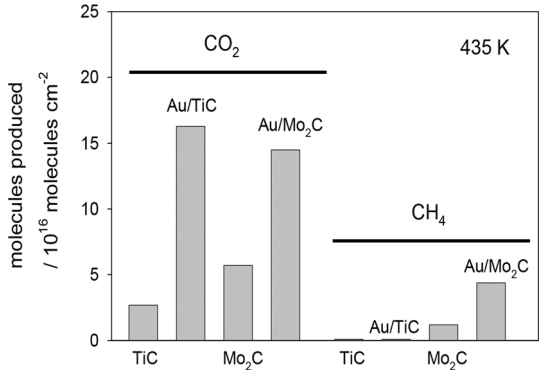

Figure 4. Production of CO_2 and CH_4 upon exposure of the catalysts TiC(001), Au/TiC(001), Mo_2C(001), and Au/Mo_2C(001) to a mixture of CO (20 Torr), H_2O (10 Torr), and H_2 (100 Torr) at 435 K for 5 min.

conversion of CO; however, the molybdenum carbide produces a significant amount of methane. The addition of Au to Mo_2C(001) produces an excellent catalyst for the conversion of CO at low temperature, but it leads simultaneously to the production of CO_2/H_2 and methane. Au/TiC(001) is the best WGS catalyst in terms of activity and selectivity (Figure 4). It is known that the 1:1 metal-to-carbon ratio in TiC(001) makes the cleavage of the C–O bond in carbon monoxide very difficult ($CO_{ads} \rightarrow C_{ads} + O_{ads}$, $\Delta E = +1.65$ eV).[9,13] This 1:1 metal-to-carbon ratio also makes TiC(001) less sensitive to the presence of water in the reaction feed.[17] After operation for 6 h, we found no signs of deactivation of the Au/TiC(001) catalyst during the WGS (see Figure S2 in the Supporting Information). In contrast, the Au/Mo_2C(0001) catalyst lost approximately 30% of its activity during the same period of time (see Figure S4). Mo_2C powders and Mo_2C(001) decompose the water molecule to form films of oxycarbides with low catalytic activity.[14,18] This deactivation process was negligible on TiC(001) and Au/TiC(001).

DFT calculations were used to study the mechanism of the WGS reaction on Au/TiC(001). First, the bonding of CO and water was examined on Au_4, Au_{13}, and Au_{29} clusters supported on a TiC(001) slab (see Figures S2 and S5). Au_{13} consisted of two layers of 9 and 4 metal atoms. Au_{29} contained three layers of 16, 9, and 4 Au atoms. Both clusters ended in a Au_4 unit, as seen in Au_4/TiC(001) (see Figure S2), but in the case of Au_{13}/TiC(001) and Au_{29}/TiC(001), the tip of the gold cluster was not in contact with the carbide substrate (see Figure S5). The strength of the bonding interactions of water with the Au clusters increased according to the sequence: $Au_{29}/TiC \approx Au_{13}/TiC \ll Au_4/TiC$, in agreement with the trend seen in our experiments for the adsorption of water on Au/TiC(001) (see Figures S1 and S3). Thus, the active sites for the WGS on Au/TiC(001) are small metal clusters in close contact with the support. A similar observation was reported for Au/oxide catalysts.[21,28]

Figure 5 compares the calculated reaction profiles for the WGS on clean TiC(001)[17] and Au_4/TiC(001). The corresponding molecular structures for the reaction intermediates and transition states are displayed in Figure 6. Our theoretical study indicated that the WGS reaction occurs preferentially at the Au sites. The optimal path for the WGS on Au/TiC(001) follows an associative mechanism in which an HOCO species is formed by the reaction of CO with an OH group produced by the dissociation of water. The formation of a key HOCO intermediate was also proposed in previous theoretical studies of the WGS on Cu(111),[32] CeO_x/Cu(111),[33] and Au/TiO_2(110).[34] Table 1 lists the calculated reaction rate constants for the main steps of the WGS on Au_4/TiC(001) as based on the DFT calculations. It is remarkable that on Au_4/TiC(001) the formation of the HOCO intermediate is an exothermic process that occurs with extremely low activation barriers, which are significantly smaller than those found on TiC(001) (0.87 eV)[17] or pure gold (>2 eV).[27] On clean TiC(001), the calculated rate constant at 300 K for the reaction CO + OH → *cis*-HOCO was only 3.20 s^{-1} per site,[17] whereas on Au_4/TiC(001) the corresponding rate was 9.63×10^7 s^{-1} per site. Surfaces of pure gold do not dissociate water.[27] In contrast, the rate constant for the dissociation of water on a Au_4 cluster supported on TiC(001) is 5.44×10^5 s^{-1} per site at 300 K. Thus, the charge polarization at the Au–TiC interface (see Figure S2)[8,25] drastically enhances the catalytic properties of gold.

A detailed comparison of the behavior of Au on TiC(001), TiO_2(110), and ZnO(000$\bar{1}$) (Figure 3) points to stronger metal–support interactions on the carbide surface. These stronger interactions make this substrate the best option for enhancing the WGS activity of Au. Charge polarization can also occur when Au is deposited on oxide surfaces,[35–37] but it is usually weaker than that seen on the TiC(001) substrate[8,25]

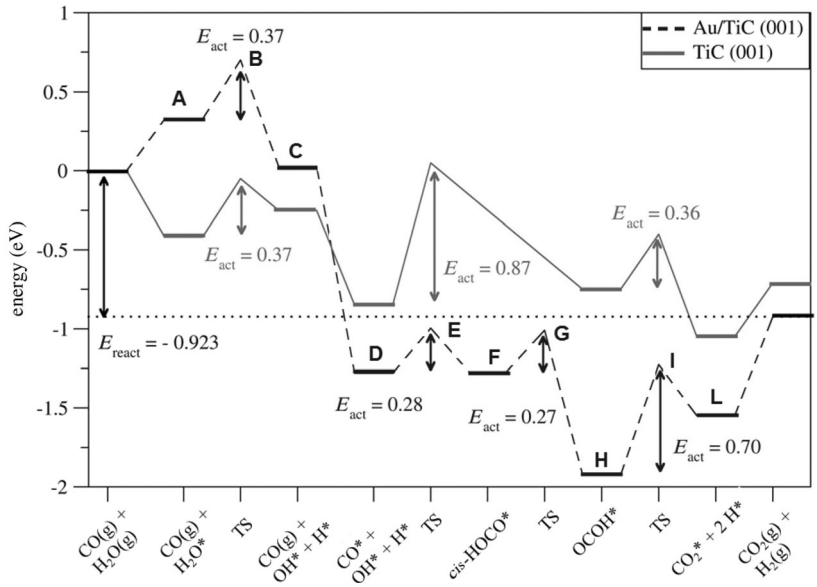

Figure 5. Energy profile derived from DFT calculations for the WGS reaction on clean TiC(001) and Au_4/TiC(001). The corresponding molecular structures are shown in Figure 6. TS = transition state.

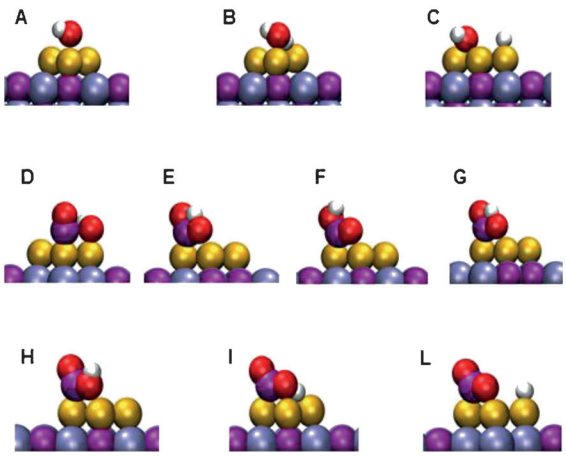

Figure 6. Molecular structures determined by DFT calculations for intermediates and transition states of the WGS on a Au_4/TiC(001) model catalyst (Au yellow, C purple, Ti gray, O red, H white). The corresponding energy profile is shown in Figure 5.

Table 1: Calculated energy barriers and rate constants for the main steps of the WGS on Au_4/TiC(001). E_{act} is given in eV per molecule and rate constants in s^{-1} per site.

Reaction	E_{act}	Rate constant (300 K)	Rate constant (450 K)
$H_2O \rightarrow OH + H$	0.37	5.44×10^{5}	6.49×10^{7}
$CO + OH \rightarrow$ *cis*-HOCO	0.28	9.63×10^{7}	5.41×10^{9}
cis-HOCO $\rightarrow$ *trans*-OCOH	0.27	1.27×10^{7}	3.70×10^{8}
$OCOH \rightarrow CO_2 + H$	0.70	1.32	1.06×10^{4}

and requires modification of the standard properties of the oxide surface. Perturbation of the electronic properties of Au is a preliminary step for the enhancement of its chemical activity, and on oxides this task can be accomplished by introducing structural or electronic defects, by creating O vacancies, and by forming $Au(OH)_x$ species.[21,28,35–37] On the other hand, the simple deposition of Au on stoichiometric TiC electronically perturbs the gold.[8,25] As a result, the interaction of Au with TiC produces a large number of active $Au(OH)_x$ species (see Figure S3) that are not present on surfaces of pure gold,[27] and the other reaction steps for the WGS proceed on the admetal at a reasonable speed. The generation of a high concentration of active $Au(OH)_x$ species probably proceeds faster on TiC(001) than on oxide surfaces, such as TiO_2(110) or MgO(001).[34] Furthermore, the 1:1 metal-to-carbon ratio in TiC provides stability and prevents the transformation of CO into methane. Thus, Au/TiC(001) is a highly active and selective catalyst for the low-temperature WGS reaction.

Experimental Section

The Au/TiC(001) and Au/Mo_2C(001) catalysts were prepared and tested in an ultrahigh vacuum chamber with an attached high-pressure cell or batch reactor.[13,30,34] Au was deposited on the metal carbide substrates by the methods described in Refs. [19,25]. The procedures for the cleaning of the TiC(001) and Mo_2C(001) surfaces are described elsewhere.[13,19,25] In the experiments, the WGS activity of the metal/carbide catalysts was tested under CO/H_2O or CO/H_2O/H_2 mixtures.[14,28,29] The CO gas was stored in aluminum tanks, and any metal-carbonyl impurities were removed by passing it through purification traps.

The periodic DFT calculations estimated exchange and correlation energy by use of the PW91-GGA[38] approximation as implemented in VASP.[39] The wave function was expanded by using a plane-wave basis set whose associated kinetic energy was lower than 415 eV. A suitable net of $3\times3\times1$ k points generated by using the Monkhorst–Pack algorithm was used to perform integration in the reciprocal space.[40] The Au_4 cluster was adsorbed on a $3(\sqrt{2}\times\sqrt{2})R45^\circ$ supercell and fully relaxed together with all adsorbates and the two upper layers of the slab until forces were smaller than 0.02 eV Å^{-1}. A vacuum with a width of about 10 Å perpendicular to the surface avoided interaction between repeated images. Transition states were identified by using the CI-NEB algorithm.[41] All structures were characterized as proper minima or saddle points by vibrational analysis. Reaction rate constants (T = 300 or 450 K) were estimated from standard transition-state theory, including the calculation of the vibrational partition function, as detailed elsewhere.[17]

Received: July 14, 2014
Published online: September 3, 2014

Keywords: gold · hydrogen production · metal–support interactions · titanium carbide · water–gas shift reaction

[1] C. T. Campbell, *Nat. Chem.* **2012**, *4*, 597 – 598.
[2] S. J. Tauster, *Acc. Chem. Res.* **1987**, *20*, 389 – 394.
[3] A. K. Datye, D. S. Kalakkad, M. H. Yao, D. J. Smith, *J. Catal.* **1995**, *155*, 148 – 153.

[4] A. Bruix, J. A. Rodriguez, P. J. Ramírez, S. D. Senanayake, J. Evans, J. B. Park, D. Stacchiola, P. Liu, J. Hrbek, F. Illas, *J. Am. Chem. Soc.* **2012**, *134*, 8968 – 8974.
[5] S. D. Senanayake, J. A. Rodriguez, D. Stacchiola, *Top. Catal.* **2013**, *56*, 1488 – 1498.
[6] N. M. Schweitzer, J. A. Schaidle, O. K. Ezekoye, X. Pan, S. Linic, L. T. Thompson, *J. Am. Chem. Soc.* **2011**, *133*, 2378 – 2381.
[7] L. K. Ono, B. Roldán-Cuenya, *Catal. Lett.* **2007**, *113*, 86 – 94.
[8] J. A. Rodriguez, F. Illas, *Phys. Chem. Chem. Phys.* **2012**, *14*, 427 – 438.
[9] A. Vidal, L. Feria, J. Evans, Y. Takahashi, P. Liu, K. Nakamura, F. Illas, J. A. Rodriguez, *J. Phys. Chem. Lett.* **2012**, *3*, 2275 – 2280.
[10] M. D. Porosoff, X. Yang, J. A. Boscoboinik, J. G. Chen, *Angew. Chem. Int. Ed.* **2014**, *53*, 6705 – 6709; *Angew. Chem.* **2014**, *126*, 6823 – 6827.
[11] A. Koós, F. Solymosi, *Catal. Lett.* **2010**, *138*, 23 – 27.
[12] S. T. Oyama, *Catal. Today* **1992**, *15*, 179 – 200.
[13] S. Posada-Pérez, F. Viñes, P. J. Ramírez, A. B. Vidal, J. A. Rodriguez, F. Illas, *Phys. Chem. Chem. Phys.* **2014**, *16*, 14912 – 14916.
[14] D. J. Moon, J. W. Ryu, *Catal. Lett.* **2004**, *92*, 17 – 24.
[15] P. M. Patterson, T. K. Das, B. H. Davis, *Appl. Catal. A* **2003**, *251*, 449 – 455.
[16] S. V. Didziulis, K. D. Butcher, *Coord. Chem. Rev.* **2013**, *257*, 93 – 109.
[17] F. Viñes, P. Liu, J. A. Rodriguez, F. Illas, *J. Catal.* **2008**, *260*, 103 – 112.
[18] P. Liu, J. A. Rodriguez, *J. Phys. Chem. B* **2006**, *110*, 19418 – 19425.
[19] J. A. Rodriguez, P. Liu, F. Viñes, F. Illas, Y. Takahashi, K. Nakamura, *Angew. Chem. Int. Ed.* **2008**, *47*, 6685 – 6689; *Angew. Chem.* **2008**, *120*, 6787 – 6791.
[20] R. B. Burch, *Phys. Chem. Chem. Phys.* **2006**, *8*, 5483 – 5500.
[21] M. Flytzani-Stephanopoulos, *Acc. Chem. Res.* **2014**, *47*, 783 – 792.
[22] K.-Z. Qi, G.-C. Wang, W.-J. Zheng, *Surf. Sci.* **2013**, *614*, 53 – 63.
[23] J.-L. Dubois, K. Sayama, H. Arakawa, *Chem. Lett.* **1992**, 5 – 8.
[24] J. Nakamura, J. M. Campbell, C. T. Campbell, *J. Chem. Soc. Faraday Trans.* **1990**, *86*, 2725 – 2734.
[25] J. A. Rodriguez, P. Liu, F. Viñes, F. Illas, Y. Takahashi, K. Nakamura, *J. Chem. Phys.* **2007**, *127*, 211102.
[26] L. K. Ono, D. Sudfeld, B. Roldán-Cuenya, *Surf. Sci.* **2006**, *600*, 5041 – 5050.
[27] P. Liu, J. A. Rodriguez, *J. Chem. Phys.* **2007**, *126*, 164705.
[28] M. Yang, L. F. Allard, M. Flytzani-Stephanopoulos, *J. Am. Chem. Soc.* **2013**, *135*, 3768 – 3771.
[29] R. Si, J. Tao, J. Evans, J.-B. Park, L. Barrio, J. C. Hanson, Y. Zhu, J. Hrbek, J. A. Rodriguez, *J. Phys. Chem. C* **2012**, *116*, 23547 – 23555.
[30] J. A. Rodriguez, P. Liu, J. Hrbek, J. Evans, M. Pérez, *Angew. Chem. Int. Ed.* **2007**, *46*, 1329 – 1332; *Angew. Chem.* **2007**, *119*, 1351 – 1354.
[31] T. P. St. Clair, S. T. Oyama, D. F. Cox, *Surf. Sci.* **2002**, *511*, 294 – 302.
[32] A. A. Gokhale, J. A. Dumesic, M. Mavrikakis, *J. Am. Chem. Soc.* **2008**, *130*, 1402 – 1414.
[33] K. Mudiyanselage, S. D. Senanayake, L. Feria, S. Kundu, A. E. Baber, J. Graciani, A. B. Vidal, S. Agnoli, J. Evans, R. Chang, S. Axnanda, Z. Liu, J. F. Sanz, P. Liu, J. A. Rodriguez, D. J. Stacchiola, *Angew. Chem. Int. Ed.* **2013**, *52*, 5101 – 5105; *Angew. Chem.* **2013**, *125*, 5205 – 5209.
[34] J. A. Rodríguez, J. Evans, J. Graciani, J.-B. Park, P. Liu, J. Hrbek, J. F. Sanz, *J. Phys. Chem. C* **2009**, *113*, 7364 – 7370.
[35] D. Ricci, A. Bongiorno, G. Pacchioni, U. Landman, *Phys. Rev. Lett.* **2006**, *97*, 036106.
[36] M. Sterrer, T. Risse, U. Martinez Pozzoni, L. Giordano, M. Heyde, H.-P. Rust, G. Pacchioni, H.-J. Freund, *Phys. Rev. Lett.* **2007**, *98*, 096107.
[37] S. Laursen, S. Linic, *J. Phys. Chem. C* **2009**, *113*, 6689 – 6693.
[38] Y. Wang, J. P. Perdew, *Phys. Rev. B* **1991**, *43*, 8911 – 8916.
[39] G. Kresse, J. Furthmüller, *Comput. Mater. Sci.* **1996**, *6*, 15 – 50.
[40] H. J. Monkhorst, J. D. Pack, *Phys. Rev. B* **1976**, *13*, 5188 – 5192.
[41] G. Henkelman, B. P. Uberuaga, H. Jónsson, *J. Chem. Phys.* **2000**, *113*, 9901 – 9904.

